Proceedings of the XVII National Conference on Superconductivity, Karpacz 2015

Superconductivity in $ThIr_2Si_2$

K. Domieracki and D. Kaczorowski*
Institute of Low Temperature and Structure Research, Polish Academy of Sciences,
P.O. Box 1410, 50-950 Wrocław, Poland

The compound $ThIr_2Si_2$ crystallizes with a tetragonal crystal structure of the $CaBe_2Ge_2$-type (space group $P4/nmm$). Its low-temperature physical properties were investigated by means of magnetization, electrical resistivity, and heat capacity measurements, performed down to 0.35 K. The experiments revealed bulk superconductivity below $T_c = 2$ K. The obtained data indicate that $ThIr_2Si_2$ is a weakly-coupled type-II BCS superconductor.

DOI: 10.12693/APhysPolA.130.593
PACS/topics: 74.25.–q, 74.70.Dd

1. Introduction

Since a few decades, intermetallics bearing lanthanoids and actinoids continue to attract much research interest due to an exceptionally wide variety in their physical properties. Amidst them, a family of ternary RT_2M_2 compounds (R = f-electron element, T = d-electron transition metal, M = Si, Ge) has received special attention owing to their intriguing low-temperature behaviors, like complex magnetic orderings or superconductivity [1, 2]. Most of these phases form as ordered derivatives of the tetragonal $BaAl_4$-type structure, namely with a body-centered $ThCr_2Si_2$-type (space group $I4/mmm$) unit cell or a primitive $CaBe_2Ge_2$-type (space group $P4/nmm$) unit cell. A few representatives of the RT_2M_2 series have been established to exhibit polymorphism. Interestingly, the polymorphs usually display distinct physical behaviors, hence providing a superb playground for advanced studies on structure–property relationships [1–4]. A remarkable observation has been made by Shelton et al. [5], who concluded from his studies on an extended series of nonmagnetic RT_2M_2 polymorphs that only those crystallizing with the $CaBe_2Ge_2$-type structure may exhibit superconductivity, while their $ThCr_2Si_2$-type counterparts always remain normal down to the lowest temperatures available. The suggested scenario has recently been confirmed for YIr_2Si_2 and $LaIr_2Si_2$ [6]. The related compound $ThIr_2Si_2$ was reported to crystallize with the $CaBe_2Ge_2$-type unit cell only [5]. According to Ref. [5], it becomes superconducting below $T_c = 2.16$–2.27 K, yet no physical data has been published to date. Hence, the main aim of the present work was to prove the electronic ground state in this material.

2. Experimental details

A polycrystalline sample of $ThIr_2Si_2$ was synthesized by arc-melting stoichiometric amounts of the elemental constituents (purity: Th — 98 wt%, Ir — 99.99 wt%, Si — 99.999 wt%) under titanium-gettered argon atmosphere. The button was turned over and remelted several times to promote homogeneity. No further heat treatment was applied.

Quality of the obtained material was checked by powder X-ray diffraction (XRD) using a PANalytical X'Pert PRO diffractometer with Cu K_α radiation. The XRD data were analyzed using the program FullProf [7]. Chemical composition of the prepared sample was verified by energy dispersive spectroscopy (EDS) employing a FEI scanning electron microscope equipped with an EDAX Genesis XM4 spectrometer.

Magnetic measurements were performed in the temperature interval from 0.5 to 3 K in applied magnetic fields up to 2 kOe using a Quantum Design MPMS SQUID magnetometer. The electrical resistivity was measured in the temperature range 0.35–300 K using a standard ac four-probes technique employing a Quantum Design PPMS platform. Electrical leads (thin copper wires) were attached to a bar-shaped specimen by spot welding. Heat capacity measurements were carried out in the temperature range 0.4–300 K in magnetic fields up to 5 kOe using a relaxation-time method implemented in a Quantum Design PPMS platform.

3. Results and discussion

The obtained XRD pattern of $ThIr_2Si_2$ is presented in Fig. 1. It was indexed within a tetragonal unit cell of the $CaBe_2Ge_2$-type (space group $P4/nmm$) with the lattice parameters: $a = 4.162$ Å and $c = 9.889$ Å, in good agreement with the literature data [8]. The EDS analysis yielded the chemical composition Th19.52Ir38.82Si41.66 (at.%) that is fairly close to the ideal one.

Figure 2 displays the temperature variation of the electrical resistivity of $ThIr_2Si_2$. The compound shows metallic behavior with the room-temperature resistivity $\rho_{RT} \approx 0.48$ mΩcm. The experimental $\rho(T)$ curve can be well approximated down to about 3 K using a parallel resistors model (PRM) [9]:

$$\frac{1}{\rho(T)} = \frac{1}{\rho_1(T)} + \frac{1}{\rho_2},$$

$$\rho_1(T) = \rho_0 + C_1 \left(\frac{T}{\Theta}\right)^3 \int_0^{\frac{\Theta}{T}} \frac{x^3\,\mathrm{d}x}{\left(1-\mathrm{e}^{-x}\right)\left(\mathrm{e}^x-1\right)}, \quad (1)$$

*corresponding author; e-mail: D.Kaczorowski@int.pan.wroc.pl

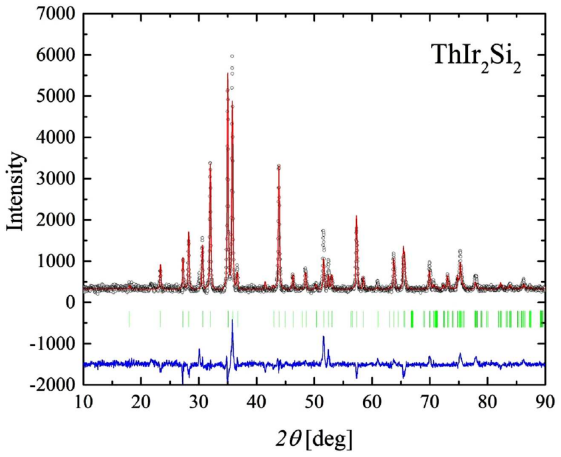

Fig. 1. Rietveld refinement (solid line) of the X-ray powder diffraction pattern of $ThIr_2Si_2$. Ticks mark the positions of the Bragg peaks.

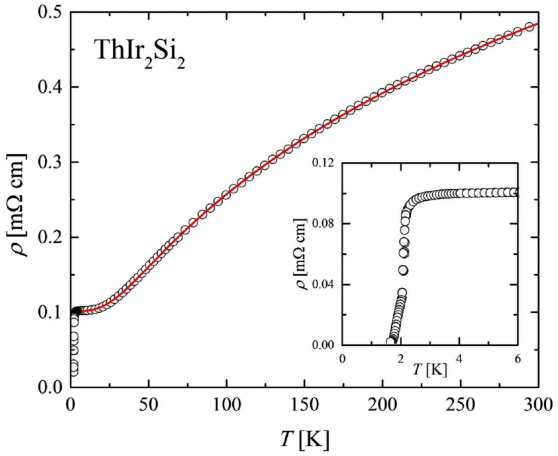

Fig. 2. Temperature dependence of the electrical resistivity of $ThIr_2Si_2$. Solid line is the PRM fit discussed in the text. Inset: low-temperature resistivity data.

where $\rho_1(T)$ represents a metallic behavior governed by the Matthiessen rule, while ρ_2 stands for the saturation resistivity in a parallel conduction channel, in which the mean free path of conduction electrons is of the order of the interatomic distances in the crystal lattice. In the former contribution, ρ_0 is the residual resistivity due to scattering conduction electrons on static defects in the crystal lattice, and the second term represents the electron–phonon scattering processes (Θ is sometimes considered as a rough measure of the Debye temperature). The PRM parameters obtained by least-squares fitting of Eq. (1) to the experimental data of $ThIr_2Si_2$ are $\rho_0 = 0.10$ mΩcm, $\Theta = 196$ K, $C_1 = 1.4$ mΩcm, and $\rho_2 = 1.05$ mΩcm. As shown in the inset to Fig. 2, near 2 K, the electrical resistivity of $ThIr_2Si_2$ suddenly decreases down to zero, marking the onset of the superconducting state, in good agreement with the literature data [5].

The superconducting ground state in $ThIr_2Si_2$ was further corroborated by the dc magnetic susceptibility results. Over a large range of temperature below 300 K, the compound was found Pauli paramagnetic with the magnetic susceptibility of about 2×10^{-4} emu/mol, yet at the lowest temperatures, a strong diamagnetic signal was observed in weak magnetic fields upon cooling the specimen in zero field (see Fig. 3b). Distinct bifurcation between the $\chi(T)$ curves taken in zero field cooling (ZFC) and field cooling (FC) regimes signals substantial pinning effect.

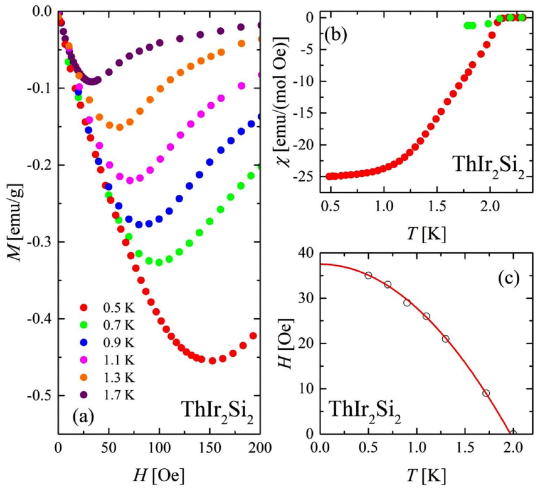

Fig. 3. (a) Magnetic field variations of the magnetization in $ThIr_2Si_2$ measured at several temperatures upon zero-field cooling. (b) Low-temperature dependences of the magnetization in $ThIr_2Si_2$ measured in a field of 10 Oe upon cooling the specimen in zero (ZFC) and applied (FC) magnetic field. (c) Temperature variation of the lower critical field in $ThIr_2Si_2$ derived from the magnetization data. Solid curve is a fitting in terms of Eq. (2).

The magnetic field variations of the magnetization in $ThIr_2Si_2$, measured at a few temperatures below 2 K upon cooling the specimen in zero magnetic field, are shown in Fig. 3a. They reveal a behavior typical for type II superconductors. Attributing the initial linear parts of the $M(H)$ isotherms to full Meissner effect, one can estimate a demagnetization factor in the sample measured to be $N_d = 0.28$. In turn, the lower critical field H_{c1} can be defined by an inflection point in the linear magnetization response. The so-obtained temperature variation of H_{c1} is plotted in Fig. 3c. The experimental results follow the standard formula [10]:

$$H_{c1}(T) = H_{c1}(0)\left[1 - \left(\frac{T}{T_c}\right)^2\right] \qquad (2)$$

with the parameters $H_{c1}(0) = 37.5$ Oe (corrected for the demagnetization) and $T_c = 1.95$ K.

The specific heat of $ThIr_2Si_2$ in the normal state is presented in Fig. 4. The value measured at room temperature is 115 J/(mol K), and thus $C(T)$ tends to ap-

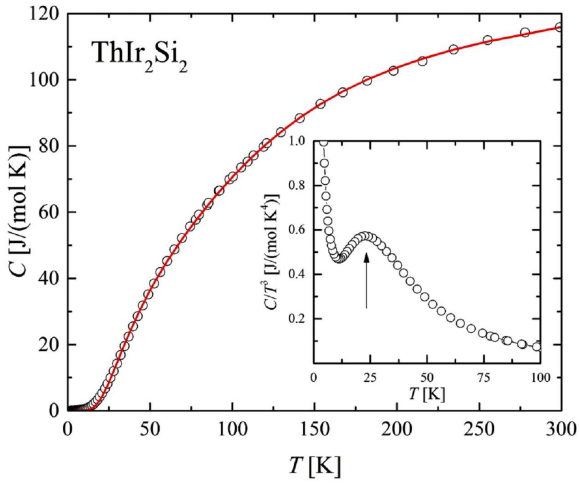

Fig. 4. Temperature variation of the specific heat of $ThIr_2Si_2$. Solid line represents the Debye–Einstein model described in the text. Inset: the specific heat data plotted as C/T^3 versus T. Arrow marks the position of a local maximum that provides an estimate for the Einstein temperature.

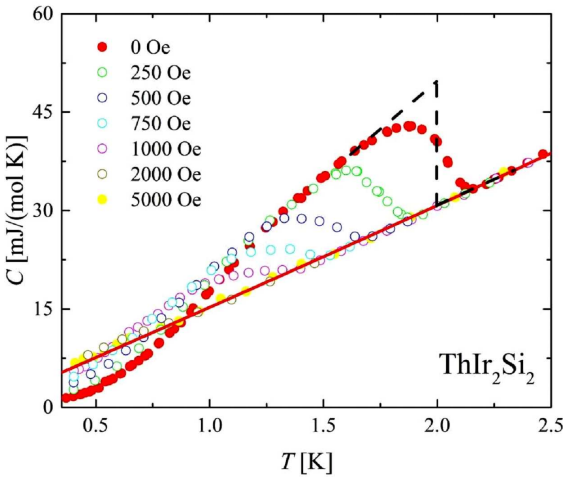

Fig. 5. Low-temperature dependences of the specific heat of $ThIr_2Si_2$ measured in zero and various applied magnetic fields. Solid curve represents the normal state fitting in terms of Eq. (4). Dashed lines depict the entropy balance near the superconducting transition in zero field.

proach the Dulong–Petit limit $3nR$ ($n = 5$ is the number of atoms per formula unit, and $R = 8.314$ J/(mol K) is the gas constant). On decreasing temperature, the specific heat approximately varies along the Debye–Einstein (DE) model [11]:

$$C(T) = \gamma T + 9nR(1-d)\left(\frac{T}{\Theta_{\rm D}}\right)^3 \int_0^{\frac{\Theta_{\rm D}}{T}} \frac{x^4 e^x}{\left(\mathrm{e}^x - 1\right)^2}\,\mathrm{d}x + 3nRd\left(\frac{\Theta_{\rm E}}{T}\right)^2 \frac{\mathrm{e}^{\Theta_{\rm E}/T}}{\left(\mathrm{e}^{\Theta_{\rm E}/T} - 1\right)^2}, \quad (3)$$

where the first term represents the electronic contribution (γ is the Sommerfeld coefficient) and the two others account for the lattice contributions ($\Theta_{\rm D}$ and $\Theta_{\rm E}$ are the Debye and Einstein temperatures, respectively, and d stands for the number of optical phonon modes). The least-squares fitting of Eq. (3) to the experimental data yielded $\gamma = 6.9$ mJ/(mol K^2), $\Theta_{\rm D} = 380$ K, $\Theta_{\rm E} = 128$ K and $d = 0.4$. Remarkably, the so-obtained value of the Einstein temperature coincides with the usual estimate $\Theta_{\rm E} \approx 5T_{\max}$ where $T_{\max}$ is a local maximum in the plot C/T^3 versus temperature (see the inset to Fig. 4).

Figure 5 displays the specific heat of $ThIr_2Si_2$ measured at low temperatures in zero and finite external magnetic field. A distinct anomaly in zero-field $C(T)$ manifests the onset of the superconducting state and proves its bulk origin. From an entropy balance (note the dashed lines in Fig. 5) one finds the specific heat jump $\Delta C = 19.4$ mJ/(mol K) at the critical temperature $T_c = 2$ K. This result implies the ratio $\Delta C/\gamma T_c = 0.67$ that is much smaller than the value of 1.43 predicted within the BCS theory for a weak-coupling superconductor. The discrepancy may be accounted for assuming the presence of some normal state regions in the superconducting matrix.

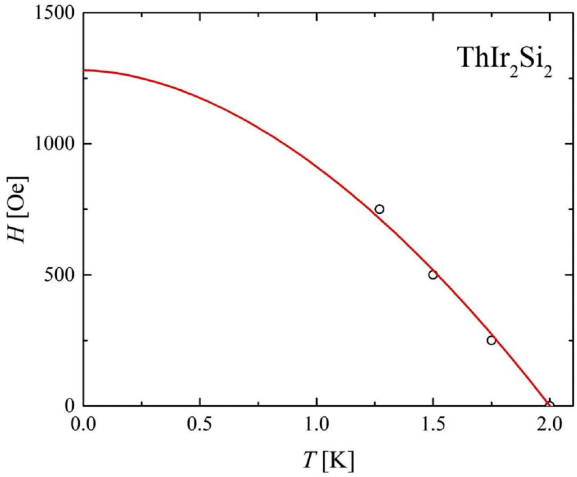

Fig. 6. Temperature variation of the upper critical field in $ThIr_2Si_2$ derived from the heat capacity data. Solid curve represents the WHH fit described in the text.

With increase of the magnitude of applied magnetic field, the anomaly in $C(T)$ shifts to lower temperatures and rapidly broadens. In a field of 5 kOe, it is not visible down to 0.4 K, and the measured $C(T)$ curve can be approximated by the Debye function

$$C(T) = \gamma T + \beta T^3 \quad (4)$$

with the parameters $\gamma = 14.5$ mJ/(mol K^2) and $\beta = 1.86 \times 10^{-4}$ J/(mol K^4). The so-obtained Sommerfeld coefficient is equal to that estimated from the high-temperature specific heat data. In turn, the Debye temperature calculated from the formula $\Theta_{\rm D} = \left(\frac{12\pi^4}{5\beta} nR\right)^{1/3}$ amounts to 373 K, which is very close to $\Theta_{\rm D}$ derived from the DE model. From the McMillan expression [12] for the electron–phonon coupling constant

$$\lambda_{ep} = \frac{1.04 + \mu^* \ln\left(\frac{\Theta_D}{1.45T_c}\right)}{(1 - 0.62\mu^*)\ln\left(\frac{\Theta_D}{1.45T_c}\right) - 1.04}, \quad (5)$$

with the Coulomb repulsion constant $\mu^* = 0.13$, one gets for $ThIr_2Si_2$ a value $\lambda_{ep} = 0.48$ appropriate for weak coupling superconductors.

Based on the $C(T)$ dependences taken in applied magnetic field, the temperature variation of the upper critical field H_{c2} was derived. As displayed in Fig. 6, the experimental data can be reasonably well described by the Werthamer–Helfand–Hohenberg theory [13] with the limiting field $H_{c2}(0) = 1.28$ kOe. The obtained value is much smaller than the Pauli limiting field $H_P = 18.6T_c = 37.2$ kOe. Applying the formula [10] $H_{c2}(0) = \frac{\Phi_0}{2\pi\xi_{GL}^2}$, where $\Phi_0 = hc/2e$ is the flux quantum, one finds for $ThIr_2Si_2$ the Ginzburg–Landau coherence length $\xi_{GL} = 50.7$ nm, and from the relationship [10] $H_{c1}(0) = \frac{\Phi_0}{4\pi\lambda_{GL}^2}\ln\left(\frac{\lambda_{GL}}{\xi_{GL}}\right)$ the penetration depth $\lambda_{GL} = 273$ nm can be calculated. These values result in the Ginzburg–Landau parameter $\kappa = \lambda_{GL}/\xi_{GL} \approx 5.4$, indicative of type-II superconductor. From the relation [10] $H_{c1}H_{c2} = H_c^2 \ln\kappa$ one obtains for the compound studied the thermodynamic critical field $H_c = 167$ Oe.

4. Conclusions

The compound $ThIr_2Si_2$ crystallizing with the tetragonal $CaBe_2Ge_2$-type structure is a bulk superconductor with $T_c = 2$ K. The main characteristics of the superconducting state indicate type-II weak-coupling superconductivity describable by the conventional BCS theory.

Acknowledgments

The study was supported by the National Science Centre (Poland) under research grant 2014/13/B/ST3/04544.

References

[1] A. Szytuła, J. Leciejewicz, in: *Handbook on the Physics and Chemistry of Rare Earths*, Vol. 12, Eds. K.A. Gschneidner, Jr., L. Eyring, North Holland, Amsterdam 1989, p 133 - 211.

[2] T. Endstra, S.A.M. Mentink, G.J. Nieuwenhuys, J.A. Mydosh, in: *Selected Topics in Magnetism*, Eds. L.C. Gupta, M.S. Multani, World Sci., Singapore 1993 p 167-198.

[3] T. Endstra, G.J. Nieuwenhuys, A.A. Menovsky, J.A. Mydosh, *J. Appl. Phys.* **69**, 4816 (1991).

[4] M. Mihalik, M. Divis, V. Sechovsky, *Physica B* **404**, 3191 (2009).

[5] R.N. Shelton, H.F. Braun, E. Musick, *Solid State Commun.* **52**, 797 (1984).

[6] M. Vališka, J. Pospíšil, J. Prokleška, M. Diviš, A. Rudajevová, V. Sechovský, *J. Phys. Soc. Jpn.* **81**, 104715 (2012).

[7] FullProf Suite 2005, version 3.30 — J. Rodriguez-Carvajal, 2005.

[8] M. Hirjak, P. Lejay, B. Chevalier, J. Etourneau, P. Hagenmuller, *J. Less-Common Met.* **105**, 139 (1985).

[9] H. Wiesmann, M. Gurvitch, H. Lutz, A. Ghosh, B. Schwarz, M. Strongin, P.B. Allen, J.W. Halley, *Phys. Rev. Lett.* **38**, 782 (1977).

[10] M. Tinkham, *Introduction to Superconductivity*, 2nd ed., Dover Books on Physics, Dover 2004.

[11] A. Tari, *The Specific Heat of Matter at Low Temperatures*, Imperial College Press, London 2003.

[12] W.L. McMillan, *Phys. Rev.* **167**, 331 (1968).

[13] N.R. Werthamer, E. Hefland, P.C. Hohenberg, *Phys. Rev.* **147**, 295 (1966).